

FIBER SEGMENTATION IN COMPOSITE MATERIALS USING MARKED POINT PROCESSES

Barna KERESZTES^{1,2}, Olivier LAVIALLE¹, Sorin POP², Monica BORDA²

(1) *Université de Bordeaux, LASIS - IMS – 351, Crs. de la Libération, 33405 Talence Cedex*

(2) *Technical University of Cluj-Napoca 15 Daicoviciu Street, 400020 Cluj-Napoca, Romania*

e-mail: barna.keresztes@ims-bordeaux.fr tel: +33 540003624

Abstract: This paper presents a new method dedicated to unsupervised 2D segmentation of fibers in a section of composite carbon-fiber materials. The framework relies on a marked point process algorithm. We shall create random elliptical objects to fit the fiber distribution in the image. The interaction rules between the objects complete the model.

Using a Markov Chain Monte Carlo (MCMC) method, the algorithm converges to a configuration which is close to the fiber distribution in the images. At each step, the configuration is evaluated considering its proximity to the target distribution. In order to achieve this task, we propose a mixed data model using both grey level values and gradients to evaluate the likelihood of the current configuration. This mixed model overcomes the problems of luminance variation, contour discontinuities and high noise level.

Finally, the results on the composite material sections illustrate the efficiency of the segmentation and suggest that the marked point processes can be a promising tool for fiber detection.

Keywords: *marked point process, composite materials, MCMC methods.*

I. INTRODUCTION

The physical properties of fibrous composites are strongly dependent on the quality of their reinforcement. Depending on the characteristics required by the application, reinforcement is carried out by weaving, stacking or needling bundles of glass or carbon fibers. The resulting fibrous structure is then densified with an appropriate matrix.

Analyzing 2D or 3D images of material samples can provide an accurate description of microstructure, particularly of the volume fiber ratio and orientation.

There are several works which threat the problem of fiber segmentation in 3D microtomography blocs [7,2]. In this case they use the spatial information and the correlation between several planes, and by knowing the orientation of the fibers their shape can be simplified to a circle with known radius in the perpendicular plane, or, in the 3D case, a cylinder.

Our goal is to detect the fibers using only the surface data that can be acquired using a microscope.

The acquisition methods used to obtain these images, and the material imperfections make it quite hard to analyze these images. The luminosity across the image varies, the contours of the individual fibers can be blurred, therefore it is difficult to implement either a pixel-based, or a contour-based method. So we propose an object-based approach where each fiber is considered an elliptical object.

It is time consuming to analyze in each pixel of the image space each possible ellipse, so a marked point process

will be proposed to achieve a fast convergence towards an optimal distribution of the objects. This algorithm is a commonly used stochastic model for simulating a set of events in space (or time). The marked point processes were first used in image segmentation by Baddeley and Van Lieshout in [1].

The paper is organized as follows: In the next section we introduce the marked point process and our object model, in section 3 we discuss the bayesian interface of the process, and in section 4 the Monte Carlo chain used for the convergence of the process will be presented.

II. MARKED POINT PROCESS

2.1 Notations

Let I be the actual image, $I=[0,w] \times [0,h]$. A configuration of objects in the image I will be noted Y . Using a marked point process X we try to approximate the observed configuration Y .

A marked point process $X=P \times K$ is a random configuration of points P in the image space, where a mark K is assigned to each point. This mark is a collection of parameters which define an object.

2.2 The object model

The images representing the composite materials contain three main regions: the fibers, the reinforced material (matrix), and the holes in the material. In this paper we are interested only in the detection of the fibers.

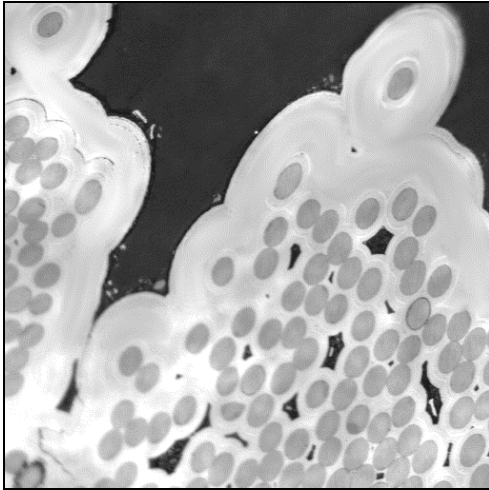


Figure 1. Microtomography image of a composite material.

A fiber is a cylindrical object, and the analyzed images represent an arbitrary section of the material. The fibers can be approximated in a 2D case either using a polygonal model or an elliptical one.

Using an elliptical model, each object is approximated with an ellipse described by five parameters: the position of the center $P(x,y)$ as the marked point, the two radii (r,R), and the inclination angle (ϕ) as the mark K .

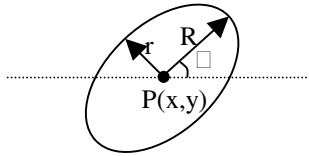


Figure 2. The object model and its parameters.

Using a more general polygonal model, we can describe more complex shapes. An n -sided polygon needs $2n$ parameters in the mark space. Thus the model is more complex, and it would have taken a much longer time to converge towards the target configuration. This model is detailed in [6].

Therefore we chose the elliptical model as the object model for the marked point process. We have observed that the real fibers have similar radii, so the parameter r , which is equal with the radius of the fiber, can be considered as constant. Thus the object space will be simplified to a subset of \mathfrak{R}^4

III. THE PROBABILITY DENSITY FUNCTION OF THE PROCESS

Let $f(X)$ be the density of a configuration X of objects, in the given image I . According to Bayes' formula, the expression of this density can be expressed as:

$$f(X) = f(X | I) \propto f_p(X) f(I | X) \quad (1)$$

The $f_p(X)$ contains all the *a priori* knowledge about the configuration, and the $f(I|X)$ the likelihood between the image and the current configuration; this will be further noted as $L(I|X)$.

3.1. The *a priori* term

We can make some restrictions on the object configuration based on the *a priori* knowledge about the shape and distribution of the objects. The first restriction we can make is that the R (long radius) parameter is greater or equal than r , we can consider it to be smaller than $2r$ (if necessary, this limit can be changed). The ϕ angle for the ellipses ranges between 0, and 2π , and we can further limit its set of values by defining a step size.

The *a priori* term can be described using the following formula:

$$f_p(X) \propto \alpha h(X) \quad (2)$$

The α function defines the probability density of the process. In this application the fibers are considered to have a homogenous Poisson distribution:

$$\alpha = \beta^{n(x)} \quad (3)$$

where β is the density of the process and $n(x)$ represents the number of objects in the configuration.

The h function defines the interaction between the different objects. Since the fibers cannot intersect, a repulsive Strauss pairwise interaction model [9] will be used, which penalizes the overlapping object configurations.

Two objects are overlapping if their silhouettes touch. This interaction will be noted \sim_o and defined by:

$$x_i \sim_o x_j \Leftrightarrow S_i \cap S_j \neq \emptyset \quad (4)$$

Since the neighboring fibers have the same orientation, there should be a correlation between their parameters. We define the correlation function as the covariance measure between the radius R and the angle ϕ of two objects:

$$C(x_i, x_j) = \text{cov}(R_i, R_j) \cdot \text{cov}(\phi_i, \phi_j) \quad (5)$$

The neighborhood relation (noted \sim_n) is defined as:

$$x_i \sim_n x_j \Leftrightarrow d(P_i, P_j) < 2(R_i + R_j) \text{ and } x_i \not\sim_o x_j \quad (6)$$

We introduce an attraction between two neighboring objects based on the correlation function $C(x_i, x_j)$

The final value of the interaction function for a given configuration X is:

$$h(X) = \prod_{x_i \sim_o x_j} \gamma \cdot \prod_{x_i \sim_n x_j} (C(x_i, x_j) + 1) \quad (7)$$

where γ is a constant, $0 < \gamma < 1$ for a repulsion between the objects; $C(i, j)$ defines the correlation between the R and \square parameters of the neighboring objects, $0 < C < 1$. The second term will be an attractive term.

In spite of the fact that in the marked point process algorithm each object should be initialized with random initial values, we can help the convergence of the process by defining the initial values (the fibers have roughly the same orientation and radii).

3.2. The data term

In this step we have to determine the probability of the existence of a configuration based on the likelihood function $L(I|X)$.

As a first approach we used the classical luminosity-based likelihood detection [8]. Two classes will be defined, the object class and the background class. A pixel belongs to the object class if it is a part of the silhouette of an object; otherwise it is considered background. The likelihood of a pixel with a class is determined using a Gaussian distribution function of the luminosities:

$$L(p|X) = \frac{1}{\sqrt{2\pi}\sigma_\varphi} e^{-\frac{(y_p - \mu_\varphi)^2}{2\sigma_\varphi^2}} \quad (8)$$

where φ denotes the class (object or background), μ_φ and σ_φ are the mean and variation of luminosities of the current class.

The likelihood of the image is the product of the pixel likelihood through the image:

$$L(I|X) = \prod_p L(p|X) \quad (9)$$

Although the material and the empty space are separable based on the grayscale value, the luminosity variation through the image makes it difficult to define a threshold between the fibers and the filling material. These two classes cannot be separated based on a Gaussian distribution of the luminosities. However we can define two classes, where one class will contain only correct detections, while some fibers which don't fall in this class won't be detected.

A gradient-based approach was considered then. This was a novelty, because it wasn't experimented yet with the marked point process, and it is difficult to define a convergent function toward the optimal solution in this case. The other issue is the presence of the gradients between the layers in the interior of the plastic material, and the gradients between the material and the empty space.

In the gradient-based likelihood detection we can't

determine the likelihood of the image conditioned by the current configuration of objects. The method used in this case is based on external fields energy, the likelihood of the individual objects is calculated and the final data term will be determined based on these values.

There are three cases of intersection between the contour of the object and the contour of a fiber in the figure 3:

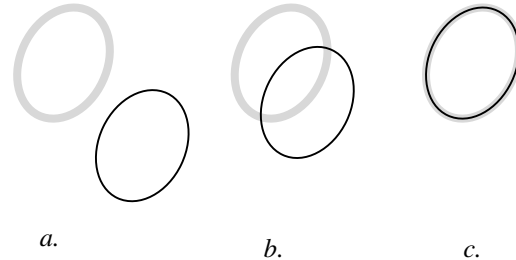


Figure 3. The different interactions between the object contour and image gradient: a. no intersection b. two common points c. identity.

Based on the intersection points it is impossible to achieve a convergence towards the solution; therefore another function will be proposed with the following properties:

- its maxima are at the contour of the detected object (maximum likelihood)
- it is monotonically increasing on each side towards these values
- outside the object the values are all positives (we accept the possibility of fiber contours outside our contour)
- close to the center of the object the values are negative (we penalize the inside contours)

There are a lot of functions which fulfill these conditions. We can use for example a truncated gaussian function, a paraboloid combined with an exponential function, a 2d function rotated around its axis, a.s.o.

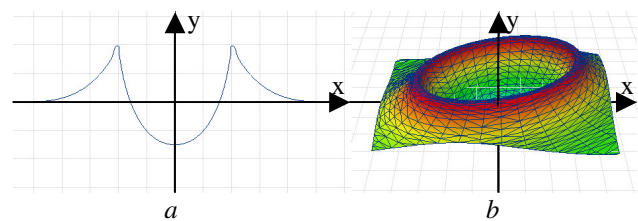


Figure 4. a. the 2D section of the proposed function b. the proposed 3D function adjusted to match the elliptical object shape.

For example, $g(x, y)$ can be described for a circular object in the following way:

$$g(x, y) = -abs \left(th - e^{-\frac{x^2 + y^2}{2\sigma^2}} \right) + th \quad (10)$$

where th is a truncation threshold. This function is later scaled and rotated to match our elliptical object using a 2 dimensional transformation matrix.

The likelihood of an object p will be the correlation between the function g and the gradient image:

$$L(x) = \int_{-n-m}^n \int_{-m}^m g(u+x, u+y) \cdot I_G(u+x, v+y) dx dy \quad (11)$$

The drawback of this approach is that the image contains many contours, between the porosity and the material, respectively between the different layers of the filling material, which have to be eliminated. Therefore we decided to combine the two methods with a voting system. Using this system, the results of the different methods could be fused to determine if the object position is probable or not. It consists on the following decision steps:

1. The objects belonging to the porosities are penalized
2. Acceptance of the objects which are likely to be a fiber based on their luminosity values
3. Acceptance of the objects with tolerated luminosity values and probable boundaries

The final likelihood value used to determine the validity of the object is determined using the likelihood values obtained in step 2. and 3.

IV. THE MCMC SIMULATION

Once we have defined the model, the next step is to create an algorithm that assures the convergence of the process towards the minimal energy of the system. Here, the energy is related to the density of a point process, so the optimal configuration is the one that maximizes this density.

$$X_{MAP} = \arg \max_X (f(X)) \quad (12)$$

In the case of marked point processes the most common method for this is the Monte Carlo Markov chain (MCMC) coupled with simulated annealing.

To simulate the MCMC, we'll use the Metropolis-Hastings-Green (MHG) algorithm [4], which was adapted by Geyer and Moller to point processes [3].

The MHG algorithm consists in proposing a new, random state y for the current state x_t . The transition kernel, noted with $q(\cdot, \cdot)$ consists in some allowed "movements"

between the two states. The allowed transitions are:

- birth (adding an object to the configuration)
- death (deleting an object)
- translation
- rotation
- dilation
- rotation and dilation combined

The algorithm can be described in the following way:

1. given the configuration x_t , we generate y using the translation kernel q .
2. we calculate the ratio between the probability of the current configuration and the proposed one:

$$r = \frac{f(y)q(y, x_t)}{f(x_t)q(x_t, y)}$$
3. with the probability $\alpha = \min(1, r)$ we accept $x_{t+1} = y$

The Metropolis-Hastings-Green algorithm

The initial configuration x_0 is considered the empty configuration.

The third step of the MHG algorithm ensures that the chain won't be struck in a local minimum of energy. The disadvantage of this approach is that the process will take a longer time to converge towards the maximum a posteriori configuration.

To optimize the chain, a simulated annealing will be introduced; $f(X)$ term will be replaced by $f^{1/T}(X)$, where T is the temperature of the system, and it is a parameter with a decreasing value towards 0.

Image name	Total fibers	Correctly detected	Misdetections	Not detected	Multiple detections	Accuracy*
5.a.	311	299	6	12	3	93.3%
5.b.	205	191	4	14	5	88.9%
5.c.	78	78	10	0	0	88%
5.d.	191	187	10	4	5	90.1%
5.e.	75	75	10	0	0	86.6%
5.f.	134	132	17	2	1	85%

* The real accuracy may be higher, because the multiple detections can be eliminated at the end of the algorithm using a simple method

Table 1. Result statistics.

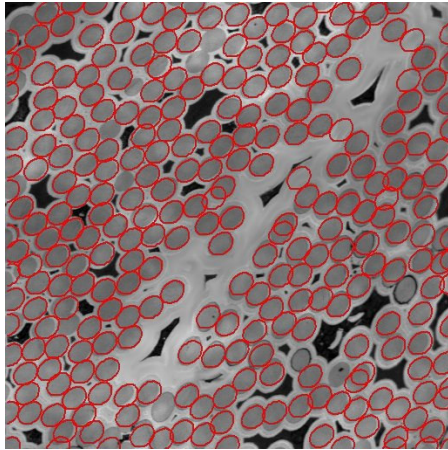


Figure 5.a.

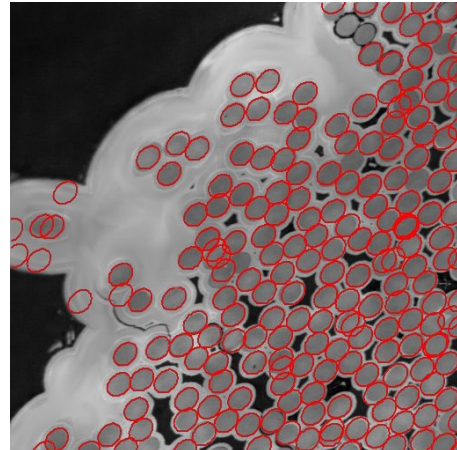


Figure 5.d.

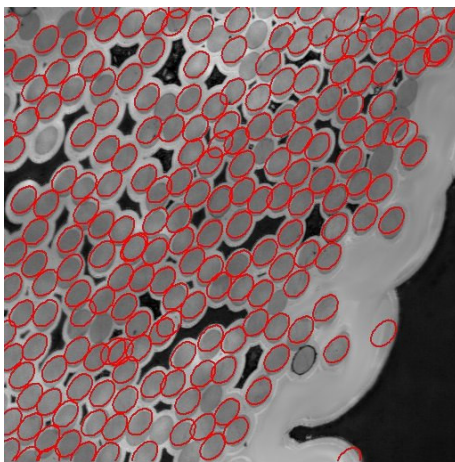


Figure 5.b.

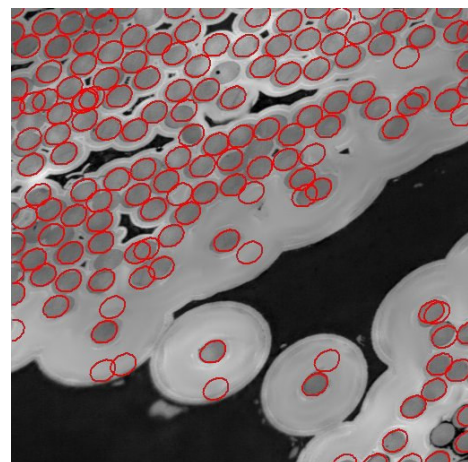


Figure 5.e.

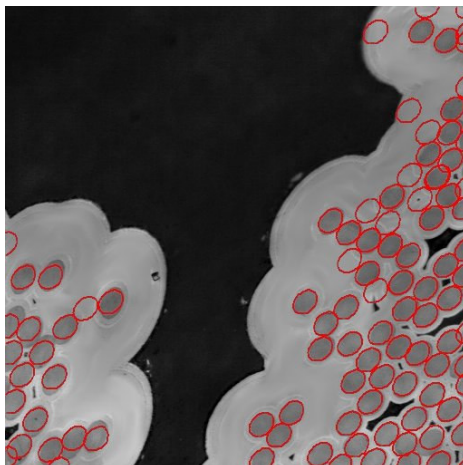


Figure 5.c.

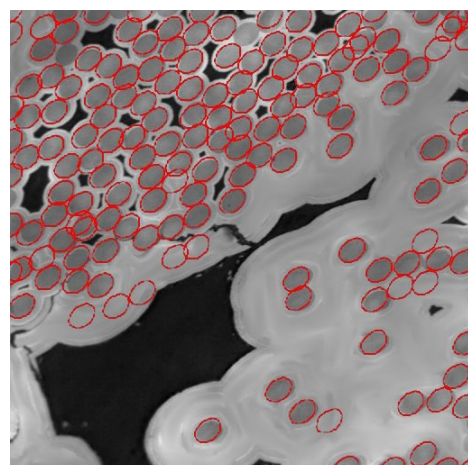


Figure 5.f.

V. RESULTS

We tested the model on microscopic and microtomography images, with a resolution of 512*512, 8 bits/pixel, greyscale.

The results are shown in fig. 5.

The Markov chain used to simulate the marked point process converges in around 100 000 steps. The process takes between 2 and 5 seconds to simulate using a Pentium 4 processor at 2.2GHz, its speed depends on the length of the chain and the number of objects. The detection accuracy was determined manually by counting the number of fibers, the correct detections and the misdetections.

As table 1. shows, the detection accuracy of the point process algorithm is around 90%.

VI. CONCLUSIONS

In this paper we presented a new kind of approach to fiber detection in composite materials using an object-based model based on the marked point process method.

In the meantime the likelihood function is also original, as the existing applications using marked point processes use only a simple approach using the pixel luminosity or homogeneity of the object silhouette. We proposed a new approach based on the image gradients, and a new decision system was created to determine the data term of a configuration.

However the algorithm accuracy still needs to be improved. A multi 2D approach is also considered for the analysis of microtomography 3D blocs, where the correlation between different sections can help improving the accuracy of the algorithm. A multi 2D algorithm for marked point processes was experimented in [5].

The authors thank the *SPS – groupe Safran* for providing data and for useful discussions.

VII. REFERENCES

- [1] A. Baddeley, M. N. M. van Lieshout, "Stochastic geometry models in high-level vision". *Statistics and Images*, 1: 231-256, 1993.
- [2] R. Blanc, C. Germain, J. P. Da Costa, P. Baylou, M. Cataldi, "Fiber orientation measurements in composite materials", *Composites Part A*, vol 37, issue 2, pp.197-206, 2006.
- [3] C. J. Geyer, J. Moller, "Simulation and likelihood inference for spatial point process", *Scandinavian Journal of Statistics, Series B*, 21, pp.359-373, 1994.
- [4] P. J. Green, "Reversible jump MCMC computation and Bayesian model determination", *Biometrika* 82, pp.711-732, 1995.
- [5] B. Keresztes, O. Lavialle, M. Borda, "Seismic fault detection based on a curvilinear support", *IGARSS 2008 Proceedings*, Boston [3], 2008.
- [6] R. Kluszczyński, M.N.M. van Lieshout, T. Schreiber, *Image segmentation with polygonal random Markov fields*, Report PNA-R0409, 2004.
- [7] C. Mulat, M. Donias, P. Baylou, G. Vignoles, C. Germain, "Optimal orientation estimators for detection of cylindrical objects", *Signal, Image and Video Processing Journal*, vol. 2, pp. 51-58, 2008.
- [8] D. J. Strauss, "A model for clustering", *Biometrika*, 62, pp. 467-475, 1975.
- [9] H. Rue, A. R. Syversveen, "Bayesian object recognition with Baddeley's delta loss", *Advances Applied Probability*, vol. 84, pp.30-64, 1998.